

Commun. Theor. Phys. **73** (2021) 115003 (16pp) https://doi.org/10.1088/1572-9494/ac2054

Transport of Jeffrey fluid in a rectangular slit of the microchannel under the effect of uniform reabsorption and a porous medium

H Mehboob[1], K Maqbool[1], R Ellahi[1,2,3,*] and Sadiq M Sait[4]

[1] Department of Mathematics and Statistics, International Islamic University, Islamabad, Pakistan
[2] Center for Modeling & Computer Simulation, Research Institute, King Fahd University of Petroleum & Minerals, Dhahran-31261, Saudi Arabia
[3] Fulbright Fellow, Department of Mechanical Engineering, University of California Riverside, United States of America
[4] Centre for Communications and IT Research, Research Institute, King Fahd University of Petroleum & Minerals, Dhahran-31261, Saudi Arabia

E-mail: rellahi@alumni.ucr.edu

Received 9 April 2021, revised 20 August 2021
Accepted for publication 24 August 2021
Published 27 September 2021

Abstract

This research explores the transport of a Jeffrey fluid through a permeable slit of microchannel under the effect of a porous medium and constant reabsorption. Physical laws of fluid mechanics are used to study the flow in a cross-sectional area of a narrow slit which generates a highly nonlinear system of partial differential equation with nonhomogeneous boundary conditions. To solve the complex boundary value problem; a recursive (Langlois) approach is used and explicit expressions for velocity, pressure, stream function, flux, shear stress and fractional reabsorption are calculated. It is noticed that the flow rate at the centre line of slit and shear stress on the walls of slit decay due to the presence of porous medium and viscoelastic fluid parameters. It is also quantitatively observed that more pressure is required for the fluid flow when the slit is filled with a porous medium and reabsorption on the walls is constant. The mathematical results of the present research have significant importance in the field of biofluid mechanics and medical industry, therefore the application of a diseased rat kidney is also included in this research: and reabsorption velocities in the case of a diseased and a healthy rat kidney are calculated with the effects of a porous medium and constant re-absorption.

Keywords: creeping flow, Jeffrey fluid, uniform re-absorption, porous medium, permeable slit, micro channel, Langlois approach

(Some figures may appear in colour only in the online journal)

Nomenclature

Symbols	Description		
u, v	Velocity components	W	Width of the rectangular slit
μ	Fluid viscosity	L	Length of the slit
V_0	Reabsorption velocity	H	Distance from centre to the wall of the slit
$Q(x)$	Axial flow rate	p	Pressure
		$\bar{p}(x)$	Mean pressure
		ψ	Stream function

* Author to whom any correspondence should be addressed.

$q(x)$	Leakage flux
ϵ	Small parameter of creeping flow
k_1	Jeffrey fluid parameters
$\Delta\bar{p}(L)$	Pressure drop
F_a	Fractional reabsorption
K_1	Permeability of porous medium
Da	Darcy's number
Q_0	Axial flow rate at the entrance region
S_1	Reabsorption rate
λ_1	Ratio of relaxation to retardation time
a	Darcy's resistance parameter
T_{wall}	Shear stress on the wall

1. Introduction

The flow-through mini and microchannels have gained significant importance in biomedical engineering, renal tubule and artificial kidneys. The main problem in the development of mini and microchannels are wall properties (friction on the surface and permeability of the wall). It is proved through the experimental results that non-Newtonian fluid flow through the slit is beneficial to improve the lubrication performance in the hydrodynamic system. Conry [1] confirmed experimentally that non-Newtonian fluid can be used for hydrodynamic viscoelastic materials and for the lubrication of rectangular contacts. Effects of load enhancement by the thickening of polymer is tested by Oliver [2] who found excellent results from his study. Spikes [3] observed the behaviour of lubricants in channels and found the pressure, velocity and flux of fluid. Sawyer and Tichy [4] used non-Newtonian lubrication for the second-order fluid, and Zhang *et al* [5] studied the same for the Maxwell fluid model. Recently, prominent scientists have studied the different non-Newtonian fluid models for the biological flows with different physical effects [6–13].

The microstructure of different types of complex fluids have gained a lot of attention due to its frequent use in the medical industry and biophysics; these fluids were characterized as viscoelastic, time-dependent and time-independent fluids [14–17]. Bird *et al* [18] proposed a theory of viscoelastic fluids that explained the viscous and elastic effects and had complex mathematical structures as well. Many interesting and challenging issues of viscoelastic fluids were discussed by Baris [19], Yamamoto *et al* [20], Nallapu and Radhakrishnamacharya [21], Reddappa *et al* [22], Mirzakhalili and Nejat [23]. An important viscoelastic fluid was a Jeffrey fluid which has a simple constitutive relation and explained the structure of viscoelastic fluid. The Jeffrey model can be used by means of local and convective derivatives of the first Rivlin Erickson tensor. Nadeem *et al* [24] discussed the similarity solution of a Jeffrey fluid over a shrinking sheet and simplified the two-dimensional momentum equation under the boundary layer assumption whereas the flow of Jeffrey fluid in a rotating frame was studied by Hayat *et al* [25]. Turkyilmazoglu [26] discussed the simultaneous effects of slip and heat transfer for Jeffrey fluid at deformable surfaces and so forth.

Fluid flow through a porous medium have gained a lot of importance in biological systems [27, 28]. Fluid transport with the help of artificial and natural porous media plays a vital role in biology, for example flow in biological tissues, fluid transport in plants in xylem and phloem etc. Therefore, many studies related to flow in porous media in biological systems are studied by Baragh *et al* [29], Farooq *et al* [30], Ajarostaghi *et al* [31], Bhatti *et al* [32] etc. From these research works, it is analysed that porous media affect the viscous and thermal properties of the non-Newtonian fluid flow [33].

In this research, a microchannel filled with a porous medium is taken to be the proximal renal tube of the diseased kidney. The two-dimensional flow of a viscoelastic fluid in a permeable rectangular conduit (two-directional) is a big challenge of the present era, and as per our knowledge, no attention has been paid to study the Darcy's number for slow flow of a viscoelastic Jeffrey fluid through a micro-channel (narrow slot) with constant reabsorption on the wall. This problem leads to a highly nonlinear set of partial differential equation with non-homogeneous boundary conditions in a finite domain. Such type of boundary value problems cannot be solved easily by numerical and analytical techniques. Analytical solution of such type of flow is important due to its fluid properties. An analytical technique which is introduced by Langlois *et al* [34] known as a recursive approach can be used to solve the slow flow of viscous fluid. Slow viscoelastic flow in an infinitely-long, straight tube of uniform cross-section was considered by Langlois and Rivlin. It was shown that the first, second, and third-order theories all predict rectilinear flow, but a fourth-order theory predicts a secondary flow in the cross-sectional area of planes. A method was outlined for calculating the first, second, and third-order flow fields and the velocity components were explicitly calculated for a rectangular slit of cross-section area. In this research two-dimensional momentum and continuity equations with the non-homogeneous boundary conditions are linearized into a steady slow flow of Jeffrey fluid in a narrow conduit with the Langlois approach.

The present research is organized into six sections. The first section includes the background and literature review of the problem. In section 2 mathematical modelling of the two-dimensional creeping flow of a Jeffrey fluid in a rectangular slit with uniform reabsorption, has been made. The recursive approach is used to solve the nonlinear problem in section 3 and expression for stream function, velocity profile, pressure distribution, shear stress on the wall, flow rate and leakage flux are calculated. The graphical results for pressure difference, velocity profile (on the entrance, middle and exit region) and stream function are presented in section 4, application of the proposed model is included in section 6 and concluding remarks are added in section 6.

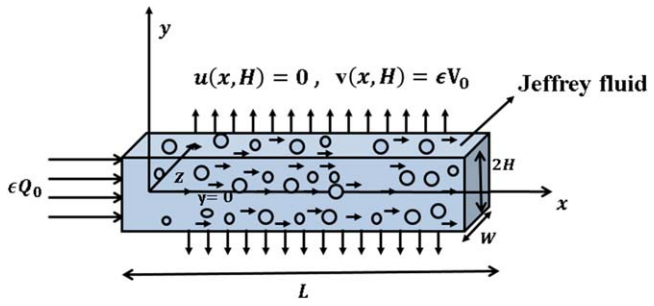

Figure 1. Geometry of the problem.

2. Mathematical modelling

Consider an incompressible, steady and two dimensional Jeffrey fluid flow through a porous medium of a rectangular cross-section of a rectangular slit with an x-axis located at the centre of the rectangular slit and y-axis in the perpendicular direction of the centreline. A constant reabsorption rate ϵV_0 at the permeable walls of the rectangular slit is uniformly distributed. The walls of the slit are separated by the distance $2H$ and the width of the slit is $W \gg H$. The volume flow rate at the entrance of the slit is ϵQ_0.

The geometry of the slit, as shown in figure 1, shows that flow is symmetric about the centreline of the slit, therefore for a computational purpose, we will consider only the upper half of the slit.

Basic equations for the creeping flow of a Jeffrey fluid [35] through a porous medium [36] are as follows

$$\nabla \cdot \boldsymbol{V} = 0, \tag{1}$$

$$\text{div}\, \boldsymbol{T} + \boldsymbol{R} = 0. \tag{2}$$

Where

$$\boldsymbol{T} = -p\boldsymbol{I} + \mathbf{S}, \tag{3}$$

$$\mathbf{S} = \frac{\mu}{1+\lambda_1}\left(1 + \lambda_2 \frac{D}{Dt}\right)\boldsymbol{A}_1, \tag{4}$$

$$\boldsymbol{A}_1 = (\text{grad}\boldsymbol{V}) + (\text{grad}\boldsymbol{V})^{\text{T}}. \tag{5}$$

Where $\boldsymbol{V}$ is the velocity field, $\boldsymbol{T}$ is the Cauchy stress tensor, $\mathbf{S}$ is the extra stress tensor, $\boldsymbol{A}_1$ is the first Rivilin Erickson tensor, $\boldsymbol{I}$ is the identity tensor, λ_1 and λ_2 are Jeffrey parameters, $\frac{D}{Dt}$ is total time derivative and $\boldsymbol{R}$ is Darcy's resistance.

As we have a porous medium therefore for evaluating $\boldsymbol{R}$ in equation (2), Darcy's law will be employed and is as follows

$$\boldsymbol{R} = -\frac{\mu}{K_1}\boldsymbol{V}.$$

The proposed problem suggests that flow through a slit has the following velocity profile

$$\boldsymbol{V} = [u(x, y), v(x, y)]. \tag{6}$$

Creeping flow through slit of micro channel is discussed by Ullah *et al* [37] and the suggest the following boundary conditions

$$u = 0, \ v = \epsilon V_0, \ \text{for}\, y = H, \tag{7}$$

$$\frac{\partial u}{\partial y} = 0, \ v = 0, \ \text{for}\, y = 0, \tag{8}$$

$$\epsilon Q_0 = 2W\int_0^H u(0, y)\text{d}y. \tag{9}$$

The creeping flow of a Jeffrey fluid through a slit suggest that inertial forces are very weak when compared with the viscous forces, therefore continuity equation and momentum equations in the absence of inertial forces are as follows:

$$\frac{\partial u}{\partial x} = -\frac{\partial v}{\partial y}, \tag{10}$$

$$\frac{\partial p}{\partial x} = \frac{\mu}{1+\lambda_1}\left[2\frac{\partial}{\partial x}\left(F_1\frac{\partial u}{\partial x} + \lambda_2 M_1\right) + \frac{\partial}{\partial y}(F_1 M_2 + \lambda_2 M_3)\right] - \frac{\mu u}{K_1}, \tag{11}$$

$$\frac{\partial p}{\partial y} = \frac{\mu}{1+\lambda_1}\left[\frac{\partial}{\partial x}(F_1 M_2 + \lambda_2 M_3) + 2\frac{\partial}{\partial y}\left(F_1\frac{\partial v}{\partial y} + \lambda_2 M_4\right)\right] - \frac{\mu v}{K_1}, \tag{12}$$

and stress components can be obtained as follows:

$$T_{xx} = -p + \frac{2\mu}{1+\lambda_1}\left[F_1\frac{\partial u}{\partial x} + \lambda_2 M_1\right], \tag{13}$$

$$T_{yx} = T_{xy} = \frac{\mu}{1+\lambda_1}[F_1 M_2 + \lambda_2 M_3], \tag{14}$$

$$T_{yy} = -p + \frac{2\mu}{1+\lambda_1}\left[F_1\frac{\partial v}{\partial y} + \lambda_2 M_4\right], \tag{15}$$

where $F_1 = (1 + \lambda_2\nabla)$ and $\nabla = u\frac{\partial}{\partial x} + v\frac{\partial}{\partial y}$.

$$M_1 = 2\left(\frac{\partial u}{\partial x}\right)^2 + \left(\frac{\partial v}{\partial x}\right)^2 + \frac{\partial v}{\partial x}\frac{\partial u}{\partial y},$$

$$M_2 = \frac{\partial u}{\partial y} + \frac{\partial v}{\partial x},$$

$$M_3 = 2\left(\frac{\partial u}{\partial x}\frac{\partial u}{\partial y} + \frac{\partial v}{\partial x}\frac{\partial v}{\partial y}\right),$$

$$M_4 = 2\left(\frac{\partial v}{\partial y}\right)^2 + \left(\frac{\partial u}{\partial y}\right)^2 + \frac{\partial v}{\partial x}\frac{\partial u}{\partial y}.$$

Non-dimensional parameters are introduced in the following form

$$x^* = \frac{x}{H}, \ y^* = \frac{y}{H}, \ u^* = \frac{u}{Q_0/WH}, \ v^* = \frac{v}{Q_0/WH}, \ p^* = \frac{p}{\mu Q_0/WH^2}, \ Da = \frac{K_1}{H^2}, \ T_{ij}^* = \frac{T_{ij}}{\mu Q_0/WH^2}. \tag{16}$$

Using equation (16) in (11)–(15) and dropping *, one can obtain the following form of equations

$$\frac{\partial u}{\partial x} = -\frac{\partial v}{\partial y}, \tag{17}$$

$$\frac{\partial p}{\partial x} = \frac{1}{1+\lambda_1}\left[2\frac{\partial}{\partial x}\left(F_2\frac{\partial u}{\partial x} + k_1 M_1\right) + \frac{\partial}{\partial y}(F_2 M_2 + k_1 M_3)\right] - \frac{u}{Da}, \tag{18}$$

$$\frac{\partial p}{\partial y} = \frac{1}{1+\lambda_1}\left[\frac{\partial}{\partial x}(F_2 M_2 + k_1 M_3) + 2\frac{\partial}{\partial y}\left(F_2\frac{\partial v}{\partial y} + k_1 M_4\right)\right] - \frac{v}{Da}, \tag{19}$$

$$T_{xx} = -p + \frac{2}{1+\lambda_1}\left[F_2\frac{\partial u}{\partial x} + k_1 M_1\right], \tag{20}$$

$$T_{yx} = T_{xy} = \frac{1}{1+\lambda_1}[F_2 M_2 + k_1 M_3], \tag{21}$$

$$T_{yy} = -p + \frac{2}{1+\lambda_1}\left[F_2\frac{\partial v}{\partial y} + k_1 M_4\right], \tag{22}$$

and boundary conditions take the following form

$$u = 0, \quad v = \epsilon S_1, \quad \text{for } y = 1, \tag{23}$$

$$\frac{\partial u}{\partial y} = 0, \quad v = 0, \quad \text{for } y = 0, \tag{24}$$

$$\int_0^1 u(0, y)\mathrm{d}y = \frac{\epsilon}{2}, \tag{25}$$

where $F_2 = (1 + k_1\nabla)$, $k_1 = \dfrac{\lambda_2 Q_0}{WH^2}$, and $S_1 = \dfrac{WHV_0}{Q_0}$ are the operator, Jeffrey parameter and reabsorption velocity respectively.

Note that when $\dfrac{1}{Da}$, λ_2, $\lambda_1 \to 0$, the above system of differential equations reduce to the creeping flow of Newtonian fluid [38].

3. Methodology

We use the Langlois recursive approach to solve the equations (18)–(19) with the boundary conditions (23)–(25).

Assume that $u(x, y)$, $p(x, y)$ and $T(x, y)$ can be expanded in the following series form:

$$u(x, y) = \sum_{i=1}^{\infty} \epsilon^i u^{(i)}(x, y),\ v(x, y) = \sum_{i=1}^{\infty} \epsilon^i v^{(i)}(x, y), \tag{26}$$

$$p(x, y) = \text{Constant} + \sum_{i=1}^{\infty} \epsilon^i p^{(i)}(x, y), \tag{27}$$

$$T(x, y) = \sum_{i=1}^{\infty} \epsilon^i T^{(i)}(x, y). \tag{28}$$

Substituting equations (26)–(28) into the (17)–(25) and equating the coefficients of ϵ, ϵ^2 and ϵ^3, one can get the following first, second and third-order problems.

3.1. First order problem

$$\frac{\partial u^{(1)}}{\partial x} = -\frac{\partial v^{(1)}}{\partial y}, \tag{29}$$

$$\frac{\partial p^{(1)}}{\partial x} = \frac{1}{1+\lambda_1}\nabla^2 u^{(1)} - \frac{u^{(1)}}{Da}, \tag{30}$$

$$\frac{\partial p^{(1)}}{\partial y} = \frac{1}{1+\lambda_1}\nabla^2 v^{(1)} - \frac{v^{(1)}}{Da},$$
$$T_{xx}{}^{(1)} + p^{(1)} = \frac{2}{1+\lambda_1}\left(\frac{\partial u^{(1)}}{\partial x}\right), \tag{31}$$

$$T_{xy}{}^{(1)} = \frac{1}{1+\lambda_1}\left(\frac{\partial v^{(1)}}{\partial x} + \frac{\partial u^{(1)}}{\partial y}\right),$$
$$T_{yy}{}^{(1)} + p^{(1)} = \frac{2}{1+\lambda_1}\left(\frac{\partial v^{(1)}}{\partial y}\right) \tag{32}$$

with the boundary conditions

$$u^{(1)} = 0,\ v^{(1)} = S_1, \text{ for } y = 1, \tag{33}$$

$$\frac{\partial u^{(1)}}{\partial y} = 0,\ v^{(1)} = 0,\ \text{for } y = 0, \tag{34}$$

$$\frac{1}{2} = \int_0^1 u^{(1)}(0, y)\mathrm{d}y \text{ for } x = 0. \tag{35}$$

Flow patterns can be observed by the stream functions; therefore stream functions can be related with the velocity profile by the following expressions:

$$u^{(1)} = \frac{\partial \psi^{(1)}}{\partial y},\ v^{(1)} = -\frac{\partial \psi^{(1)}}{\partial x}. \tag{36}$$

With the help of the above stream function, the first-order problem takes the following form.

$$\nabla^4 \psi^{(1)} - a^2\nabla^2\psi^{(1)} = 0. \tag{37}$$

$$\frac{\partial \psi^{(1)}}{\partial y} = 0,\ \frac{\partial \psi^{(1)}}{\partial x} = -S_1, \quad \text{for } y = 1, \tag{38}$$

$$\frac{\partial^2 \psi^{(1)}}{\partial y^2} = 0,\ \frac{\partial \psi^{(1)}}{\partial x} = 0, \quad \text{for } y = 0, \tag{39}$$

$$\psi^{(1)}(0, 0) = 0, \quad \psi^{(1)}(0, 1) = \frac{1}{2}. \tag{40}$$

To solve the above boundary value problem by inverse method, the following function is defined:

$$\psi^{(1)}(x, y) = S_1 x X^{(1)}(y) + Y^{(1)}(y). \tag{41}$$

After using the above expression, equations (37)–(40) take the following form

$$\frac{\mathrm{d}^4X^{(1)}}{\mathrm{d}y^4} - a^2\frac{\mathrm{d}^2X^{(1)}}{\mathrm{d}y^2} = 0, \tag{42}$$

$$\frac{\mathrm{d}}{\mathrm{d}y}X^{(1)}(y) = 0,\ X^{(1)}(y) = -1, \quad \text{at } y = 1, \tag{42a}$$

$$\frac{\mathrm{d}^2}{\mathrm{d}y^2}X^{(1)}(y) = 0,\ X^{(1)}(y) = 0, \quad \text{at } y = 0. \tag{42b}$$

The solution of equation (42) is given by the following expression

$$X^{(1)}(y) = A_1 + A_2 y + A_3\mathrm{e}^{ay} + A_4\mathrm{e}^{-ay}. \tag{43}$$

After using the boundary conditions given in equations (42*a*) and (42*b*) one can get the following values of arbitrary constants

$$A_1 = 0,\ A_2 = -2A_3 a\cosh a,\ A_4 = -A_3,$$
$$A_3 = \frac{1}{2(a\cosh a - \sinh a)}. \tag{44}$$

After using the values of arbitrary constants one can get the exact solution of $X^{(1)}$ that is given in appendix.

$$\frac{\mathrm{d}^4Y^{(1)}}{\mathrm{d}y^4} - a^2\frac{\mathrm{d}^2Y^{(1)}}{\mathrm{d}y^2} = 0, \tag{45}$$

$$\frac{\mathrm{d}}{\mathrm{d}y}Y^{(1)}(y) = 0,\ Y^{(1)}(y) = \frac{1}{2},\ \text{at } y = 1, \tag{45a}$$

$$\frac{\mathrm{d}^2}{\mathrm{d}y^2}Y^{(1)}(y) = 0,\ \ Y^{(1)}(y) = 0,\ \ \text{at } y = 0, \tag{45b}$$

where $a^2 = \dfrac{1+\lambda_1}{Da}$.

Following the same procedure of $X^{(1)}$ one can get the solution of the above equation is given as follows:

$$Y^{(1)}(y) = B_1 + B_2 y + B_3\mathrm{e}^{ay} + B_4\mathrm{e}^{-ay}. \tag{46}$$

After using the boundary conditions given in equations (45*a*) and (45*b*) one can get the following values of arbitrary constants

$$B_1 = 0,\ B_2 = -2B_3 a\cosh a,\ \ B_4 = -B_3,\ \ B_3 = \frac{-1}{4(a\cosh a - \sinh a)}. \tag{47}$$

After using the values of arbitrary constants one can get the exact solution of $Y^{(1)}$ that is given in an appendix.

Following formulae are used to find mean pressure at any section of the slit and pressure drop of slit respectively.

$$\bar{p}^{(1)}(x) = \int_0^1 (p^{(1)} - {p_0}^{(1)})\mathrm{d}y, \tag{48}$$

$$\Delta\bar{p}^{(1)}(L) = \bar{p}^{(1)}(0) - \bar{p}^{(1)}(L). \tag{49}$$

3.2. Second-order problem

After equating coefficients of ϵ^2, the following equations are obtained with the corresponding boundary conditions

$$\frac{\partial u^{(2)}}{\partial x} = -\frac{\partial v^{(2)}}{\partial y}, \tag{50}$$

$$\frac{\partial p^{(2)}}{\partial x} = \frac{1}{1+\lambda_1}\nabla^2 u^{(2)} + \frac{k_1}{1+\lambda_1}\left[2\frac{\partial}{\partial x}N_1 + \frac{\partial}{\partial y}N_2\right] - \frac{u^{(2)}}{Da}, \tag{51}$$

$$\frac{\partial p^{(2)}}{\partial y} = \frac{1}{1+\lambda_1}\nabla^2 v^{(2)} + \frac{k_1}{1+\lambda_1}\left[\frac{\partial}{\partial x}N_2 + 2\frac{\partial}{\partial y}N_3\right] - \frac{v^{(2)}}{Da}, \tag{52}$$

$${T_{xx}}^{(2)} + p^{(2)} = \frac{2}{1+\lambda_1}\left[\frac{\partial u^{(2)}}{\partial x} + k_1 N_1\right], \tag{53}$$

$${T_{xy}}^{(2)} = \frac{1}{1+\lambda_1}[{M_2}^{(2)} + k_1 N_2], \tag{54}$$

$${T_{yy}}^{(2)} + p^{(2)} = \frac{2}{1+\lambda_1}\left(\frac{\partial v^{(2)}}{\partial y} + k_1 N_3\right), \tag{55}$$

where

$$\nabla^{(1)} = u^{(1)}\frac{\partial}{\partial x} + v^{(1)}\frac{\partial}{\partial y},$$
$$N_1 = \nabla^{(1)}\frac{\partial u^{(1)}}{\partial x} + {M_1}^{(1)},$$
$$N_2 = \nabla^{(1)}{M_2}^{(1)} + {M_3}^{(1)},$$
$$N_3 = \nabla^{(1)}\frac{\partial v^{(1)}}{\partial y} + {M_4}^{(1)}.$$

Boundary conditions for second order problem are as follow

$$u^{(2)} = 0, \quad v^{(2)} = 0, \quad \text{for } y = 1, \tag{56}$$

$$\frac{\partial u^{(2)}}{\partial y} = 0, \quad v^{(2)} = 0, \quad \text{for } y = 0, \tag{57}$$

$$0 = \int_0^1 u^{(2)}(0, y)\mathrm{d}y \text{ for } x = 0. \tag{58}$$

Stream function for a second-order problem is given as follow

$$u^{(2)} = \frac{\partial\psi^{(2)}}{\partial y}, \quad v^{(2)} = -\frac{\partial\psi^{(2)}}{\partial x}. \tag{59}$$

After using the above relation, equations (51) and (52) together with boundary conditions take the following form

$$\nabla^4\psi^{(2)} - a^2\nabla^2\psi^{(2)} = -\frac{a^5 k_1 S_1(-1 + 2S_1 x)\cosh(a)}{2(-a\cosh(a) + \sinh(a))^2} \times (ay\cosh(ay) - \sinh(ay)), \tag{60}$$

$$\frac{\partial\psi^{(2)}}{\partial y} = 0, \quad \frac{\partial\psi^{(2)}}{\partial x} = 0, \quad \text{for } y = 1, \tag{61}$$

$$\frac{\partial^2\psi^{(2)}}{\partial y^2} = 0, \quad \frac{\partial\psi^{(2)}}{\partial x} = 0, \quad \text{for } y = 0, \tag{62}$$

$$\psi^{(2)}(0,0)=0, \quad \psi^{(2)}(0,1)=0. \tag{63}$$

A solution of the above boundary value problem can be assumed as

$$\psi^{(2)}=-\frac{a^5k_1S_1(-1+2S_1x)\cosh(a)}{2(-a\cosh(a)+\sinh(a))^2}X^{(2)}(y). \tag{64}$$

With the aid of above relation, equations (60)–(63) reduce into following form

$$\frac{\mathrm{d}^4X^{(2)}}{\mathrm{d}y^4}-a^2\frac{\mathrm{d}^2X^{(2)}}{\mathrm{d}y^2}=ay\cosh(ay)-\sinh(ay), \tag{65}$$

$$\frac{\mathrm{d}}{\mathrm{d}y}X^{(2)}(y)=0, \quad X^{(2)}(y)=0, \quad \text{for } y=1, \tag{66}$$

$$\frac{\mathrm{d}^2}{\mathrm{d}y^2}X^{(2)}(y)=0, \quad X^{(2)}(y)=0, \quad \text{for } y=0. \tag{67}$$

The solution of the above nonhomogeneous differential equation is the sum of a complementary and particular solution.

$$X^{(2)}(y)=X_c{}^{(2)}(y)+X_p{}^{(2)}(y),$$

here $X_c{}^{(2)}=0$, because boundary conditions are homogeneous and $X_p{}^{(2)}(y)$ is given as follow

$$\begin{aligned}&X_p{}^{(2)}(y)\\&=\frac{2ay(6+\cosh(2a))+14y\cosh(ay)(-a\cosh(a)+\sinh(a))-7y\sinh(2a)}{8a^3(a\cosh(a)-\sinh(a))}\\&\quad+\frac{2a(a(-1+y^2)\cosh(a)-(-6+y^2)\sinh(a))\sinh(ay)}{8a^3(a\cosh(a)-\sinh(a))}.\end{aligned}$$

where

$$\begin{aligned}N_4&=\nabla^{(1)}\frac{\partial u^{(2)}}{\partial x}+\nabla^{(2)}\frac{\partial u^{(1)}}{\partial x}\\&\quad+4\frac{\partial u^{(1)}}{\partial x}\frac{\partial u^{(2)}}{\partial x}+\frac{\partial v^{(1)}}{\partial x}M_2{}^{(2)}+\frac{\partial v^{(2)}}{\partial x}M_2{}^{(1)},\\N_5&=\nabla^{(1)}M_2{}^{(2)}+\nabla^{(2)}M_2{}^{(1)}\\&\quad+2\left(\frac{\partial u^{(1)}}{\partial x}\frac{\partial u^{(2)}}{\partial y}+\frac{\partial u^{(2)}}{\partial x}\frac{\partial u^{(1)}}{\partial y}\right.\\&\quad\left.+\frac{\partial v^{(1)}}{\partial x}\frac{\partial v^{(2)}}{\partial y}+\frac{\partial v^{(2)}}{\partial x}\frac{\partial v^{(1)}}{\partial y}\right),\\N_6&=\nabla^{(1)}\frac{\partial v^{(2)}}{\partial y}+\nabla^{(2)}\frac{\partial v^{(1)}}{\partial y}\\&\quad+4\frac{\partial v^{(1)}}{\partial y}\frac{\partial v^{(2)}}{\partial y}+M_2{}^{(1)}\frac{\partial u^{(2)}}{\partial y}+M_2{}^{(2)}\frac{\partial u^{(1)}}{\partial y},\end{aligned}$$

and boundary conditions are

$$u^{(3)}=0, \quad v^{(3)}=0, \quad \text{for } y=1, \tag{74}$$

$$\frac{\partial u^{(3)}}{\partial y}=0, \quad v^{(3)}=0, \quad \text{for } y=0, \tag{75}$$

3.3. Third-order problem

After comparing the powers of ϵ^3, one can get the following expressions

$$\frac{\partial u^{(3)}}{\partial x}=-\frac{\partial v^{(3)}}{\partial y}, \tag{68}$$

$$\begin{aligned}\frac{\partial p^{(3)}}{\partial x}&=\frac{1}{1+\lambda_1}\nabla^2u^{(3)}+\frac{k_1}{1+\lambda_1}\left[2\frac{\partial}{\partial x}N_4+\frac{\partial}{\partial y}N_5\right]\\&\quad-\frac{u^{(3)}}{Da},\end{aligned} \tag{69}$$

$$\begin{aligned}\frac{\partial p^{(3)}}{\partial y}&=\frac{1}{1+\lambda_1}\nabla^2v^{(3)}+\frac{k_1}{1+\lambda_1}\left[\frac{\partial}{\partial x}N_5+2\frac{\partial}{\partial y}N_6\right]\\&\quad-\frac{v^{(3)}}{Da},\end{aligned} \tag{70}$$

$$T_{xx}{}^{(3)}+p^{(3)}=\frac{2}{1+\lambda_1}\left[\frac{\partial u^{(3)}}{\partial x}+k_1N_4\right], \tag{71}$$

$$T_{xy}{}^{(3)}=\frac{1}{1+\lambda_1}\left[\frac{\partial u^{(3)}}{\partial y}+\frac{\partial v^{(3)}}{\partial x}+k_1N_5\right], \tag{72}$$

$$T_{yy}{}^{(3)}+p^{(3)}=\frac{2}{1+\lambda_1}\left[\frac{\partial v^{(3)}}{\partial y}+k_1N_6\right], \tag{73}$$

$$0=\int_0^1 u^{(3)}(0,y)\mathrm{d}y \text{ for } x=0. \tag{76}$$

Now stream function for a third-order problem is related in the following manner.

$$u^{(3)}=\frac{\partial\psi^{(3)}}{\partial y}, \quad v^{(3)}=-\frac{\partial\psi^{(3)}}{\partial x}, \tag{77}$$

with the help of above relation, equations (69)–(70) with the boundary conditions take the following form

$$\begin{aligned}&\nabla^4\psi^{(3)}-a^2\nabla^2\psi^{(3)}=(-1+2S_1x)\\&B_1(B_2y+(B_3y+B_4y^3)\cosh(ay)\\&\quad+(B_5+B_6y^2)\sinh(ay)+B_7\sinh(2ay)).\end{aligned} \tag{78}$$

The associated boundary conditions are

$$\frac{\partial\psi^{(3)}}{\partial y}=0, \quad \frac{\partial\psi^{(3)}}{\partial x}=0, \quad \text{for } y=1, \tag{79}$$

$$\frac{\partial^2\psi^{(3)}}{\partial y^2}=0, \quad \frac{\partial\psi^{(3)}}{\partial x}=0, \quad \text{for } y=0, \tag{80}$$

$$\psi^{(3)}(0,0)=0, \ \psi^{(3)}(0,1)=0. \tag{81}$$

From equation (78), we can assume the following solution.

$$\psi^{(3)} = (-1 + 2S_1x)B_1X^{(3)}(y), \tag{82}$$

where $X^{(3)}(y)$ represent an unknown function.

With the aid of above stream function, equations (78)–(81) transform into the following form

$$\frac{\mathrm{d}^4X^{(3)}}{\mathrm{d}y^4} - a^2\frac{\mathrm{d}^2X^{(3)}}{\mathrm{d}y^2} = B_2y + B_3y\cosh(ay) + B_4\sinh(ay) + B_5y^3\cosh(ay) + B_6y^2\sinh(ay) + B_7\sinh(2ay), \tag{83}$$

$$\frac{\mathrm{d}}{\mathrm{d}y}X^{(3)}(y) = 0, \quad X^{(3)}(y) = 0, \quad \text{at } y = 1, \tag{84}$$

$$\frac{\mathrm{d}^2}{\mathrm{d}y^2}X^{(3)}(y) = 0, \quad X^{(3)}(y) = 0, \quad \text{at } y = 0. \tag{85}$$

Follow the same steps as of second-order system, one can get the value of $X^{(3)}(y)$ by computing the complementary and particular solution that is given in the appendix.

After collecting the first, second and third-order solutions, one can get the stream function, velocity and pressure which are also given in the appendix

$$\begin{aligned}
&\psi = \psi^{(1)} + \psi^{(2)} + \psi^{(3)},\\
&p - p_0 = p^{(1)} + p^{(2)} + p^{(3)},\\
&u = u^{(1)} + u^{(2)} + u^{(3)},\\
&v = v^{(1)} + v^{(2)} + v^{(3)}.
\end{aligned} \tag{86}$$

The pressure drop of the slit is calculated by the following formula and is given in an appendix

$$\Delta\bar{p}(L) = \bar{p}(0) - \bar{p}(L). \tag{87}$$

Wall shear stress can be calculated by the following formula

$$T_{\mathrm{wall}} = T_{xy}|_{y=1}. \tag{88}$$

Fractional reabsorption is defined as

$$\begin{aligned}
F_a &= \frac{Q(0) - Q(L)}{Q(0)}.\\
&= 2LS_1.
\end{aligned} \tag{89}$$

The axial flow rate is as follow

$$\begin{aligned}
Q(x) &= 2\int_1^0 u(x, y)\mathrm{d}y,\\
&= 1 - 2S_1x.
\end{aligned} \tag{90}$$

Leakage flux is defined as follows

$$q(x) = -\frac{\mathrm{d}Q}{\mathrm{d}x} = 2S_1. \tag{91}$$

Note that fractional reabsorption and leakage flux both depend upon reabsorption rate (S_1) but pressure distribution, velocity and stress components depend upon reabsorption rate (S_1), Darcy's number (Da) and Jeffrey parameters k_1 and λ_1.

Equations (11)–(12) contain the term $\frac{1}{K_1}$ due to porous medium, if $\frac{1}{K_1} \to 0$, then one can attain the results of creeping flow of Jeffrey fluid through a slit presented by Mehboob *et al* [35].

3.4. Special case for viscous fluid

From equations (18)–(19) one can get the results of viscous fluid when Jeffrey parameters $k_1(\lambda_2)$ and $\lambda_1 \to 0$ and Darcy's number $1/Da \to 0$ then the second and third-order system of present research give the trivial solution. The solution for velocity profiles, pressure gradient and shear stress of the special case can only be obtained from the first-order system which are as follows:

$$\begin{aligned}
u &= \lim_{a\to 0}\frac{(-1 + 2S_1x)(-a\cosh(a) + a\cosh(ay))}{2a\cosh(a) - 2\sinh(a)}\\
&= \frac{3}{4}(1 - 2S_1x)(1 - y^2),
\end{aligned} \tag{92}$$

$$v = \lim_{a\to 0}\frac{S_1(ay\cosh(a) - \sinh(ay))}{a\cosh(a) - \sinh(a)} = \frac{S_1}{2}(3y - y^3), \tag{93}$$

$$p - p_0 = \frac{3[(1 - S_1x)x - S_1y^2]}{2}. \tag{94}$$

4. Graphical illustrations

Graphical behaviour of horizontal and vertical component of velocity, flow rate, pressure difference, stream function and wall shear stress are observed for distinct values of porosity parameter S_1 , Jeffrey parameters k_1, λ_1 and Darcy's number Da. In this study $x = 0.1$, $x = 0.5$ and $x = 0.9$, show the middle and exit points of the rectangular cross-section respectively.

4.1. Effect of porosity parameter (S_1)

Figures 2(a)–(c) indicate that horizontal velocity decreases by increasing the porosity parameter S_1 at the entry, middle and exit region of rectangular cross-section, a decrease is faster in the middle region but at the exit, region reverse flow has been observed. It is also observed that near the centre of rectangular cross-section flow is maximum due to pressure gradient and near the walls of a rectangular cross-section, the fluid flow becomes stationary due to wall friction. The variation of porosity parameter S_1 for the magnitude of the vertical component of velocity is shown in figure 6(a) which indicates that the vertical velocity component is symmetric about the centre line also increases by increasing S_1. Figure 7(a) display

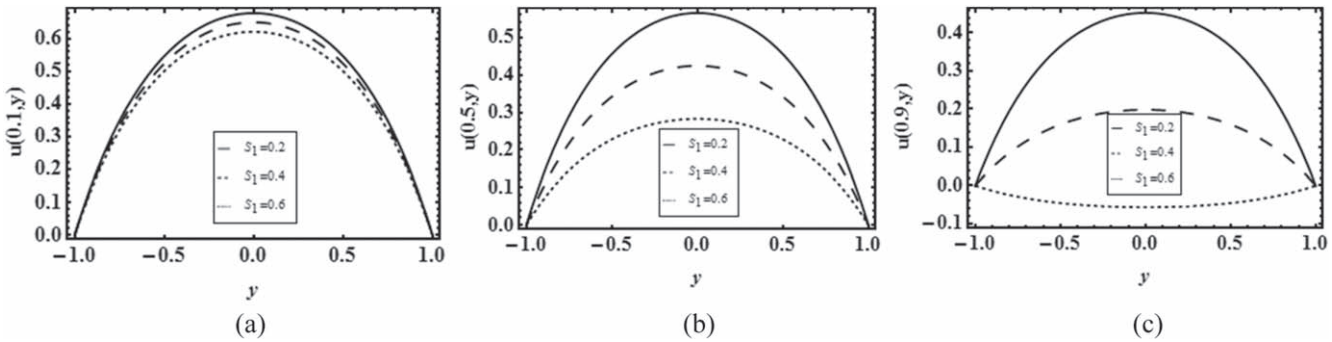

Figure 2. Effect of S_1 on horizontal velocity component for $k_1 = 0.4$, $\lambda_1 = 1.2$ and $Da = 0.5$.

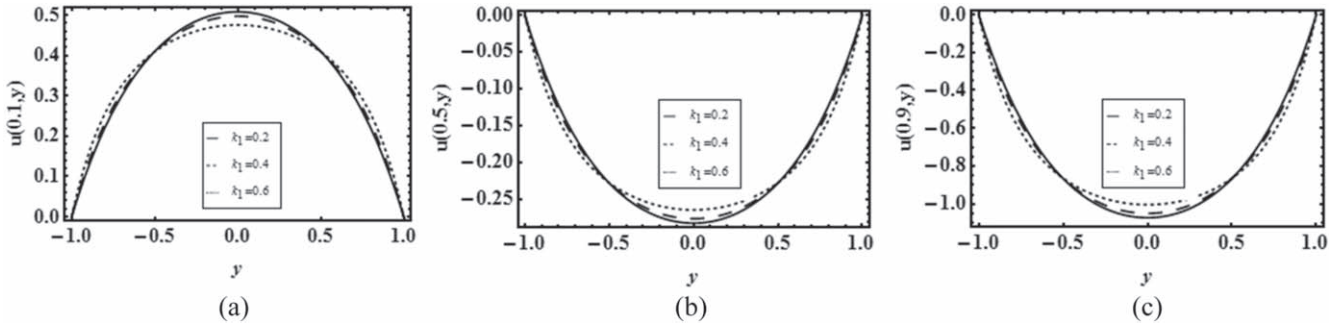

Figure 3. Effect of k_1 on horizontal velocity component for $S_1 = 1.4$, $\lambda_1 = 1.2$ and $Da = 0.5$.

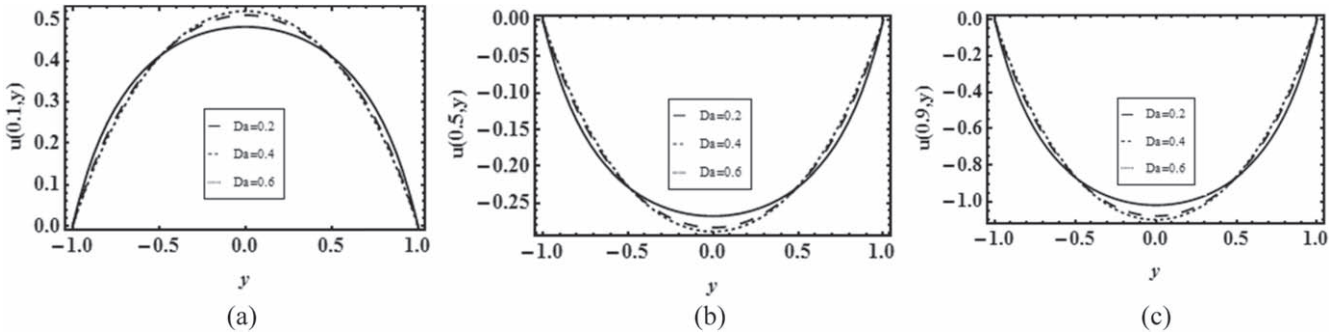

Figure 4. Effect of Da on horizontal velocity component for $S_1 = 1.4$, $\lambda_1 = 0.2$ and $k_1 = 0.4$.

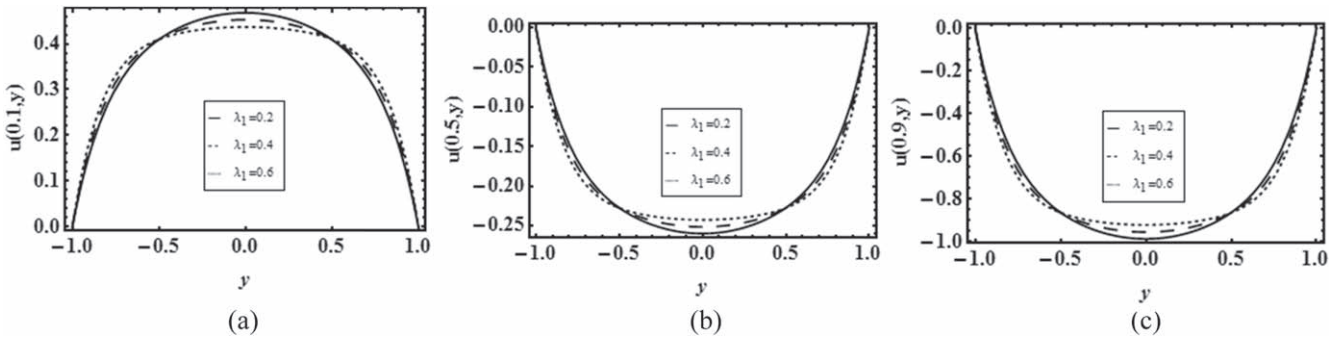

Figure 5. Effect of λ_1 on horizontal velocity component for $k_1 = 1.2$, $Da = 0.6$ and $S_1 = 1.4$.

that more pressure is required to make the fluid flow in a slit when the reabsorption rate S_1 rises. Due to high reabsorption, more pressure is required for the fluid to flow. Figure 8(a) indicates that the porosity parameter causes a reduction in the shear stress on the wall, therefore fluid moves with less amount of tangential force along the wall. From figure 9 it is observed that the volume flow rate reduces by increasing the reabsorption velocity because reabsorption velocity is transverse to the flow direction. The streamlines are shown in figures 10(a)–(c). It can be noticed that by increasing the

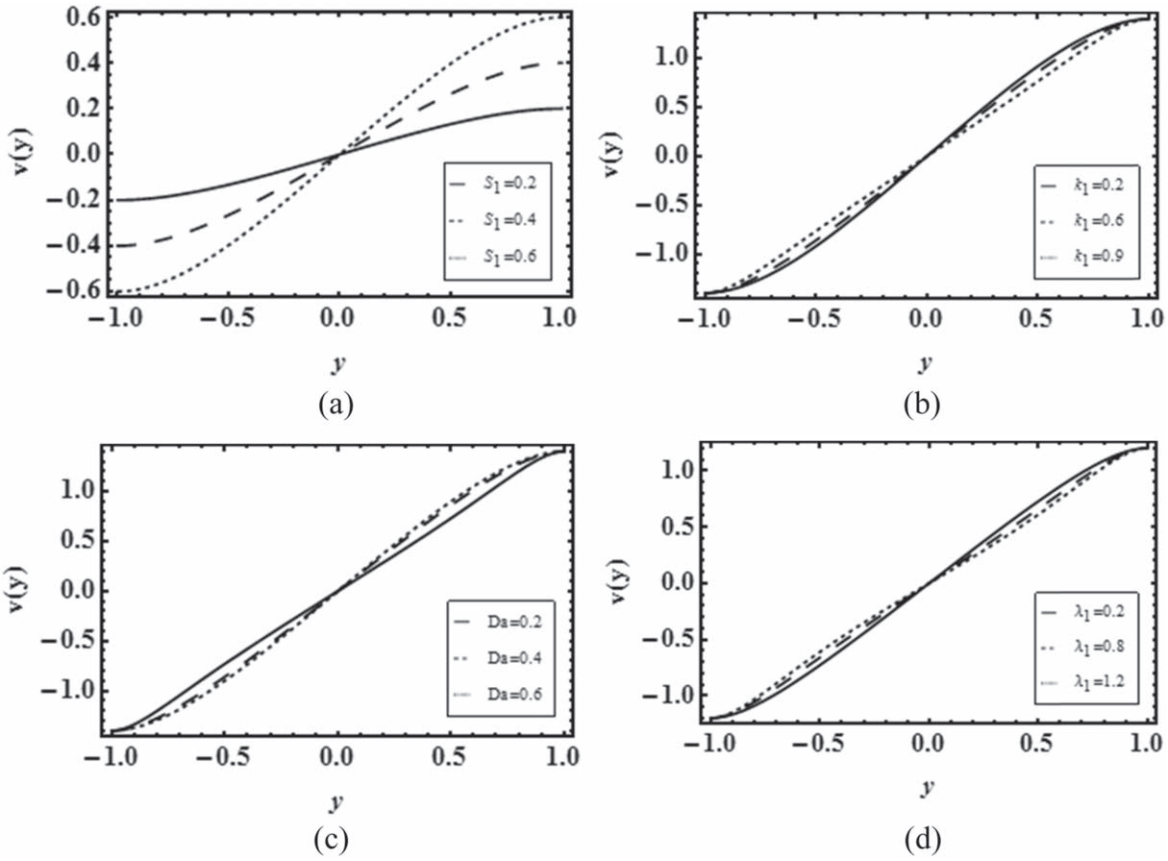

Figure 6. Effect of S_1, k_1, Da and λ_1 on vertical velocity component.

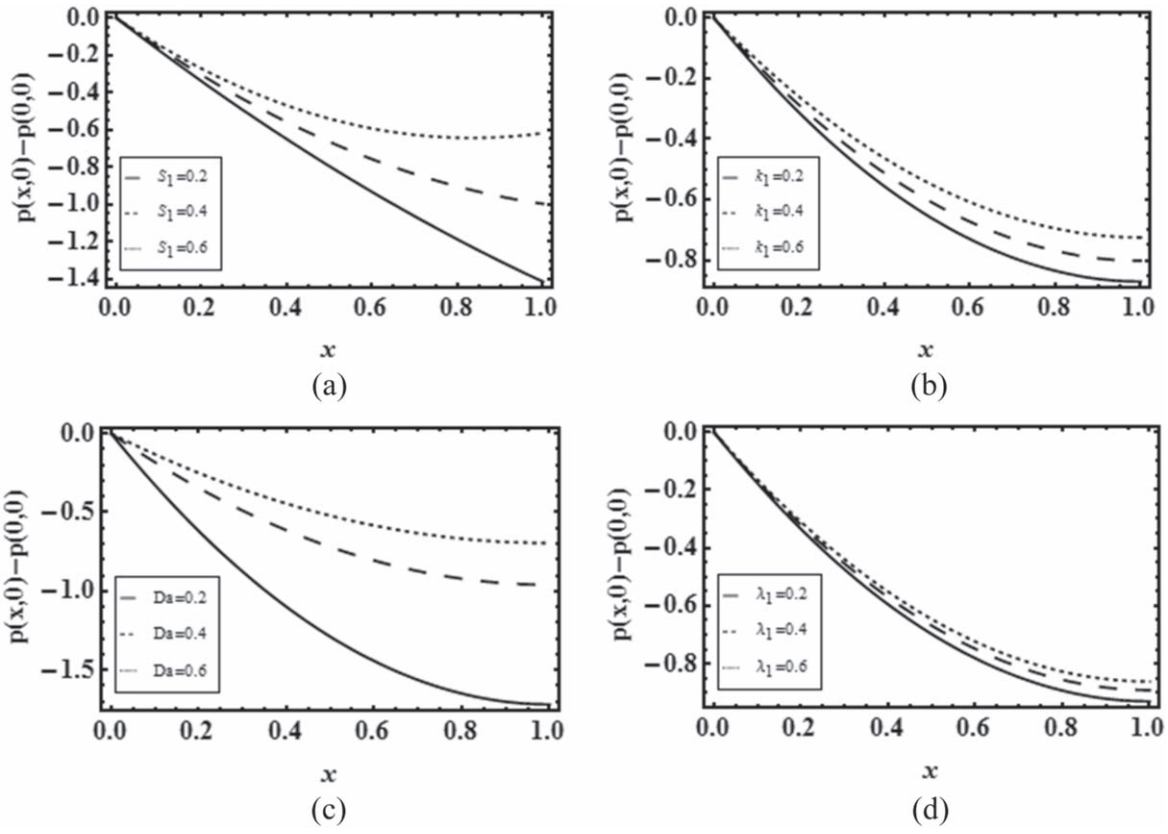

Figure 7. Effect of S_1, k_1, Da and λ_1 on the pressure difference.

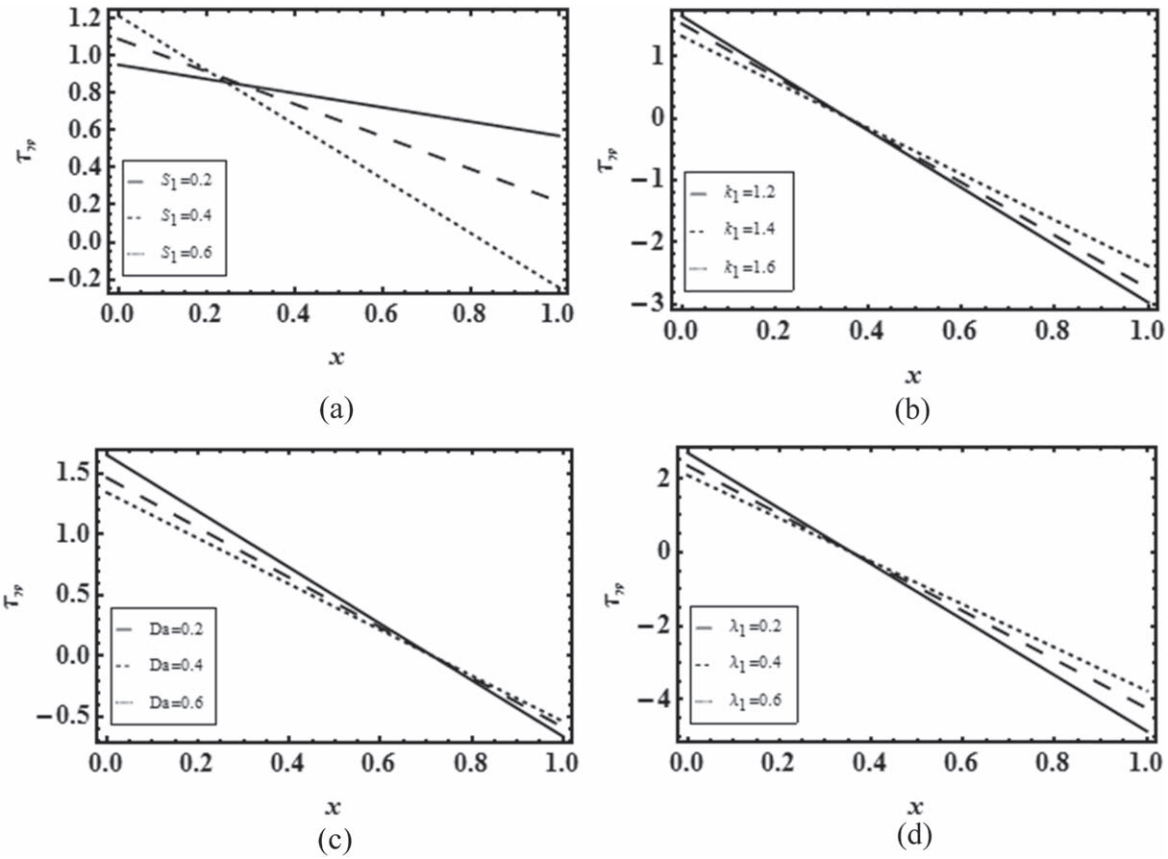

Figure 8. Effect of S_1, k_1, Da and λ_1 on shear stress on the wall.

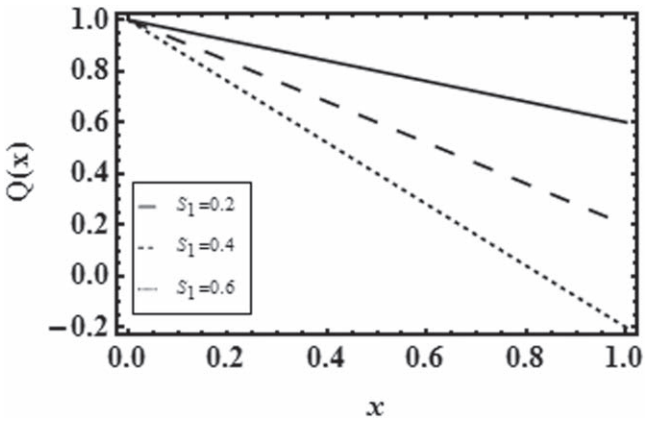

Figure 9. Effect of S_1 on axial flow rate.

values of porosity parameter S_1 the contour size increases which predicts that reabsorption causes thinning of fluid.

4.2. Effect of Jeffrey parameter (k_1) and ratio of relaxation to retardation times (λ_1)

Figures 3(a)–(c) and 5(a)–(c) show the effect of Jeffrey parameters k_1 and λ_1 for the velocity profile at the entrance, middle and exit region of the slit. The impact of Jeffrey parameters k_1 and λ_1 on the vertical component of velocity can be seen in figures 6(b) and (d). It is observed that the magnitude of vertical velocity decreases by increasing Jeffrey fluid parameters k_1 and λ_1, For distinct values of k_1 and λ_1. Figures 7(b) and (d) show that amount of pressure from one point to another point falls with the extending amount of viscosities k_1 and λ_1 of the Jeffrey fluid. Figures 8(b) and (d) illustrate that increasing Jeffrey fluid parameters k_1 and λ_1 help to decrease the wall shear stress. The streamlines are shown by the graphs of stream function in figures 11(a)–(c) and 13(a)–(c). Figures 11(a)–(c) indicate that by increasing Jeffrey fluid parameter k_1, contour size decreases due to viscoelastic properties of the fluid whereas figures 13(a)–(c) show that with the increasing values of λ_1 (ratio of relaxation to the retardation time) contour size increases because the relaxation time exceeds the retardation time.

4.3. Effect of Darcy's number (Da)

It can be seen from figures 4(a)–(c) that by increasing Darcy's number Da horizontal velocity increases in the middle of the rectangular cross-section and decreases near the wall. In the middle and exit region of the rectangular cross-section, the reverse flow has been observed due to finite boundary. Figure 6(c) describes that with the increasing values of Darcy's number Da transverse component of velocity increases as pore size in the bulk of fluid increases. Figure 7(c) shows that pressure difference decreases by increasing Da. The impact of Da on wall shear stress is shown in Figure 8(c), which indicates that shear stress decreases with the increase in Da. Figures 12(a)–(c) illustrates the effect of Da on streamlines and it can be noticed that contour size decreases as Da rises.

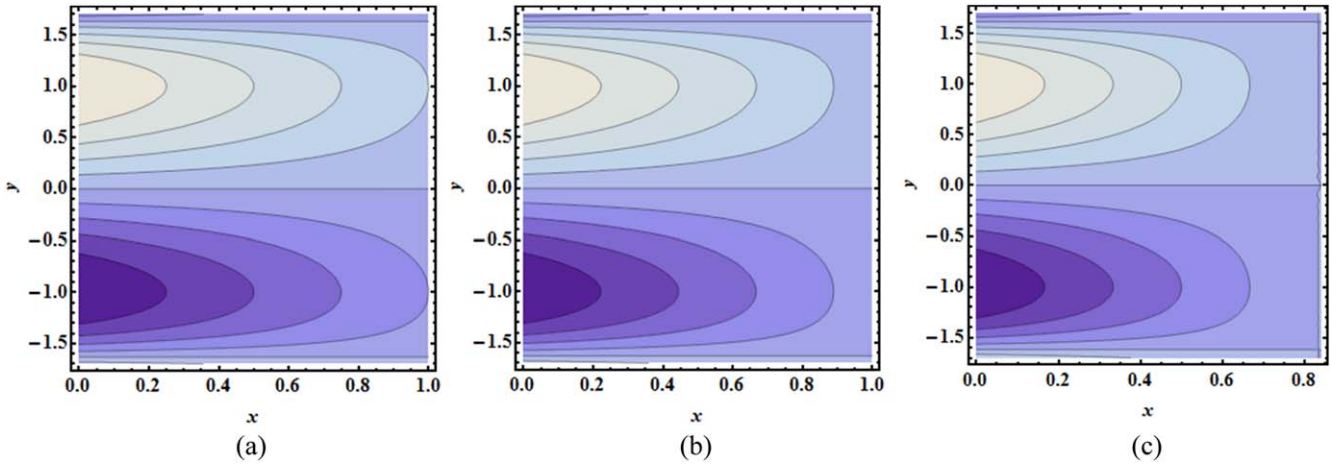

Figure 10. Effect of S_1 on stream function (a) $S_1 = 0.4$, (b) $S_1 = 0.45$, (c) $S_1 = 0.6$.

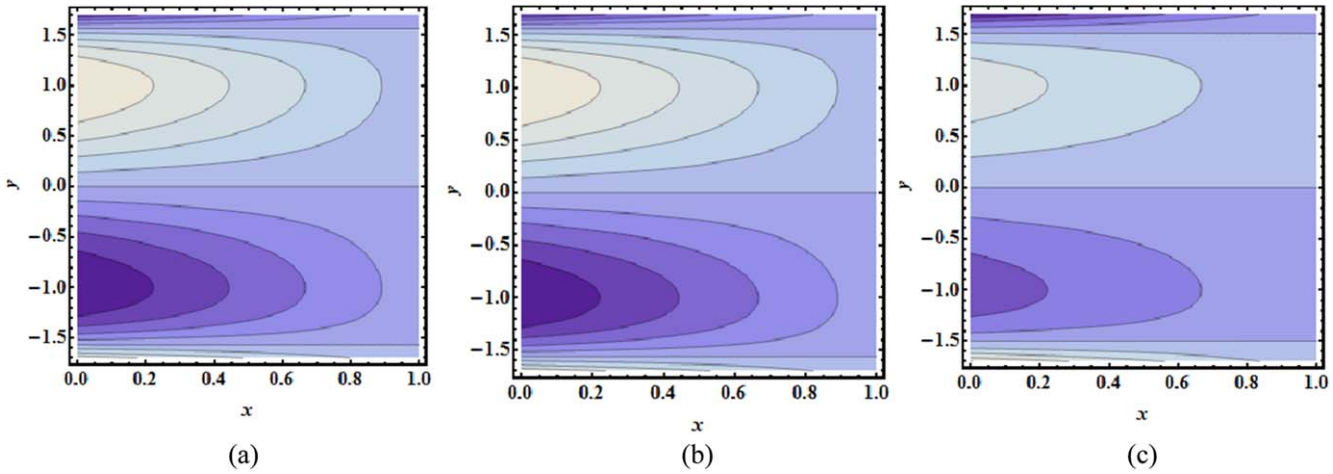

Figure 11. Effect of k_1 on stream function (a) $k_1 = 0.15$, (b) $k_1 = 0.4$, (c) $k_1 = 0.9$.

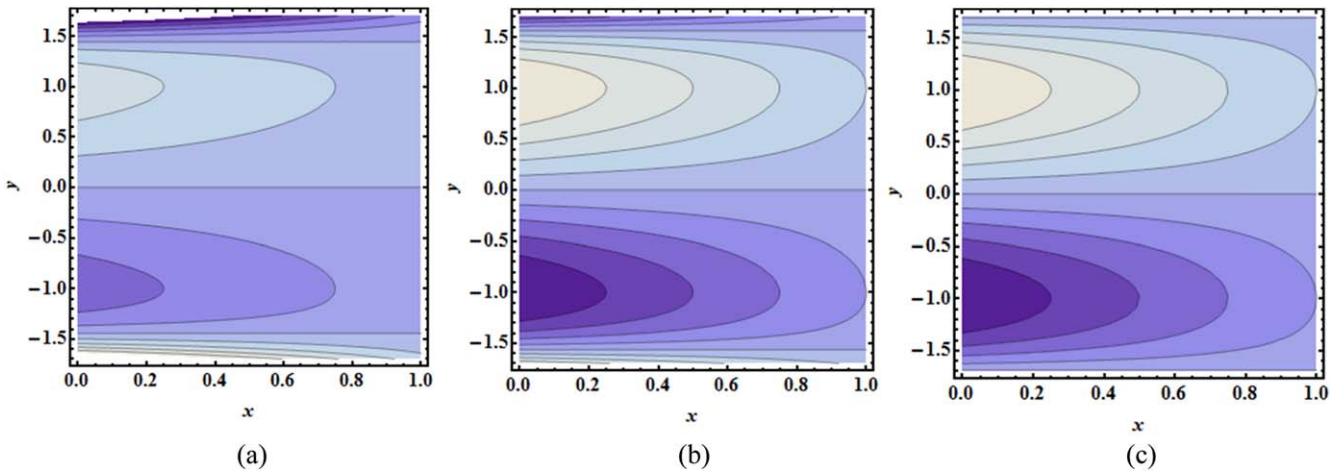

Figure 12. Effect of Da on stream function (a) $Da = 0.1$, (b) $Da = 0.3$, (c) $Da = 2.0$.

5. Application to the diseased kidney

Fifty years ago, renal transplantation of a rat was performed. Although at that time the microsurgical technique was challenging, several combinations of a genetic and outbred rats were used to model many complications of renal transplantation, including IRI, acute rejection and chronic allograft nephropathy. When the renal tubule is infected by the pus cells then the urine contains small pus cells that are considered as pores in the bulk of the fluid volume. Results of this research i.e. equation (94) is used

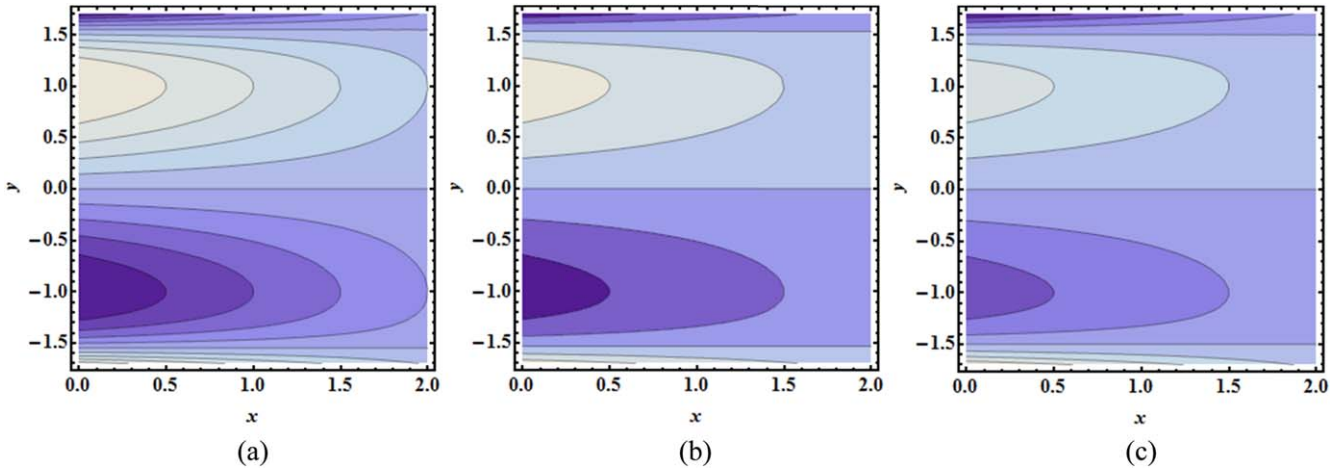

Figure 13. Effect of λ_1 on stream function (a) $\lambda_1 = 0.3$, (b) $\lambda_1 = 0.5$, (c) $\lambda_1 = 1.0$.

Table 1. Filtration rate for the diseased rat kidney (in the presence of Darcy's resistance).

Fractional reabsorption	80%	70%	60%	50%
Average pressure (dyne cm^{-2})	1.6×10^4	1.3×10^4	1.0×10^4	7.6×10^3
Filtration rate (cm s^{-1})	2.3×10^{-4}	2.0×10^{-4}	1.7×10^{-4}	1.4×10^{-4}

Table 2. Derived values from the present model for a healthy kidney.

Description	Symbol	Numerical value
Pressure drop	∇p	15 mmHg
Reabsorption rate	V_0	5.638×10^{-4} cm s^{-1}

to evaluate the average pressure and filtration rate in the diseased rat kidney. Tables 1–2 show that for different values of fractional reabsorption, average pressure and filtration rate give significant results. It is assumed from the literature [39] that $L = 0.67$ cm, $H = 0.001\,08$ cm, $W = 10^{-1}$ cm, $\mu = 0.007\,37$dyn s cm^{-2}, $Q_0 = 4.08 \times 10^{-8}$ cm^3 s^{-1}, $\lambda_1 = 0.1$ and $\lambda_2 = 0.0321$ can be used in the results of equation (94) to find the average pressure and filtration rate of the rat kidney. For computing Darcy's number, we have chosen the values of K_1 from [40]. Table 1 shows that with the increase in fractional reabsorption and filtration rate, fluid requires high pressure when compared with the healthy kidney. The average values of pressure required for the urine flow and reabsorption of the different substances during the urine formation through the healthy kidney are given in table 2. This study is very helpful to measure the pressure and fractional reabsorption required during the blood filtration through an artificial kidney.

6. Conclusions

In the present study, the slow flow of a Jeffrey fluid through a permeable rectangular slit of cross-sectional area $L \times W \times H$ embedded in a porous medium is discussed. The mathematical model of creeping flow of a Jeffrey fluid is presented by the set of the complicated nonlinear partial differential equation which is solved by the Langlois approach. The results of [38] for the case of Newtonian fluid can be obtained, if λ_1, $\lambda_2 \to 0$ and $k_1 \to 0$ whereas and the results of Mehboob *et al* [35] recovers as a special case when one choose $k_1 \to 0$. The present research analyses different features for velocity, pressure and stream functions, which are as follows

- The axial velocity diminishes with the extending values of porosity parameter S_1 in the rectangular cross-section of the slit, and also there is a decrease in axial velocity, which is dominant in the middle region of the slit and reverse behaviour is observed at the exit of a slit.
- It is predicted that mounted values of Jeffrey parameters (k_1, λ_1) cause shrinkage in the magnitude of axial velocity at the centre of the entrance, middle and exit region.
- The magnitude of transverse velocity grows with the extending values of S_1 and Da and decays with the improving values of k_1 and λ_1 but at the centre of slit, the fluid comes at rest and then start to move in the opposite direction.
- It is also noticed that more pressure is required to flow the fluid in a slit when the reabsorption rate S_1 rises but the amount of pressure from one point to another falls with the extending amount of viscosities k_1 and λ_1.
- The present research indicates that the porosity parameter cause reduction in shear stress on the wall because uniform reabsorption helps to accelerate the flow, and therefore, the fluid moves with less amount of tangential force along the wall.
- The volume flow rate of Jeffrey fluid through the slit reduces by increasing the reabsorption velocity because reabsorption velocity is transverse to the flow direction.

- The contour size increases by increasing the values of porosity parameter S_1 and Darcy number Da which show that reabsorption causes thinning of the Jeffrey fluid and increasing value of Jeffrey fluid parameters k_1 and λ_1 show that the contour size decreases which causes to thickening of the Jeffrey fluid.

This research is beneficial to measure the pressure, flow rate, and reabsorption of the urine flow through a diseased kidney. The present study has neglected the effects of body forces, inertial forces and curvature that can be considered in future work.

Acknowledgments

We thank the reviewers for their constructive suggestions which led to an improvement in this research.

Funding information

There is no funding source for this research.

Conflict of interest

On behalf of all authors, the corresponding author states that there is no conflict of interest.

Appendix

$$X^{(1)}(y) = \frac{-ay\cosh(a) + \sinh(ay)}{a\cosh(a) - \sinh(a)}$$

$$Y^{(1)}(y) = \frac{X^{(1)}(y)}{2}$$

$$\psi^{(1)} = \frac{(-1 + 2S_1x)X^{(1)}(y)}{2}$$

$$u^{(1)} = \frac{(-1 + 2S_1x)(-a\cosh(a) + a\cosh(ay))}{2a\cosh(a) - 2\sinh(a)}$$

$$v^{(1)} = -S_1X^{(1)}(y)$$

$$p^{(1)} = \frac{a^2(x(-1 + S_1x) - S_1y^2)(1 + \lambda_1)\cosh(a) + 2S_1(1 - a^2Da + \lambda_1)\cosh(ay)}{2aDa(1 + \lambda_1)(\mathrm{acosh}(a) - \sinh(a))} + {p_0}^{(1)}$$

where ${p_0}^{(1)}$ is the pressure at the entrance of the slit and $a = \sqrt{\frac{1 + \lambda_1}{Da}}$.

$$\bar{p}^{(1)}(x) = \frac{a^3(-3x + S_1(-1 + 3x^2))(1 + \lambda_1)\cosh(a) + 6S_1(-1 + a^2Da - \lambda_1)(a - \sinh(a))}{6a^2Da(1 + \lambda_1)(\mathrm{acosh}(a) - \sinh(a))}$$

$$\Delta\bar{p}^{(1)}(L) = -\frac{aL(-1 + LS_1)\cosh(a)}{2Da(\mathrm{acosh}(a) - \sinh(a))}$$

$${T_{xx}}^{(1)} = -{p_0}^{(1)} + \frac{a^2(-4DaS_1 + x(1 + \lambda_1) - S_1(x^2 - y^2)(1 + \lambda_1))\cosh(a)}{2aDa(1 + \lambda_1)(\mathrm{acosh}(a) - \sinh(a))} + \frac{2S_1(-1 + 3a^2Da - \lambda_1)\cosh(ay)}{2aDa(1 + \lambda_1)(\mathrm{acosh}(a) - \sinh(a))}$$

$${T_{xy}}^{(1)} = \frac{a^2(-1 + 2S_1x)\sinh(ay)}{(1 + \lambda_1)(2\mathrm{acosh}(a) - 2\sinh(a))}$$

$$T_{yy}{}^{(1)} = -p_0{}^{(1)} + \frac{a^2(4DaS_1 + x(1+\lambda_1) - S_1(x^2-y^2)(1+\lambda_1))\cosh(a)}{2aDa(1+\lambda_1)(\text{acosh}(a) - \sinh(a))} - \frac{2S_1(1+a^2Da+\lambda_1)\cosh(ay)}{2aDa(1+\lambda_1)(\text{acosh}(a) - \sinh(a))}$$

$$T_{xx}{}^{(1)} - T_{yy}{}^{(1)} = \frac{4aS_1(\cosh(a) - \cosh(ay))}{(1+\lambda_1)(-\text{acosh}(a) + \sinh(a))}$$

$$X^{(2)}(y) = \frac{2ay(6+\cosh(2a)) + 14y\cosh(ay)(-a\cosh(a) + \sinh(a)) - 7y\sinh(2a)}{8a^3(a\cosh(a) - \sinh(a))} + \frac{2a(a(-1+y^2)\cosh(a) - (-6+y^2)\sinh(a))\sinh(ay)}{8a^3(a\cosh(a) - \sinh(a))}$$

$$\psi^{(2)} = \frac{a^2k_1S_1(-1+2S_1x)\cosh(a)(-2ay(6+\cosh(2a)) + 14ycosh(ay)(\text{acosh}(a) - \sinh(a)))}{16(\text{acosh}(a) - \sinh(a))^3} + \frac{a^2k_1S_1(-1+2S_1x)\cosh(a)(2a(-a(-1+y^2)\cosh(a) + (-6+y^2)\sinh(a))\sinh(ay))}{16(\text{acosh}(a) - \sinh(a))^3} + \frac{7a^2k_1S_1(-1+2S_1x)\cosh(a)y\sinh(2a)}{16(\text{acosh}(a) - \sinh(a))^3}$$

$$u^{(2)} = -\frac{A_1(a(6+\cosh(2a)) - 7\cosh(a)\sinh(a) + 5ay(-\text{acosh}(a) + \sinh(a))\sinh(ay))}{8(\text{acosh}(a) - \sinh(a))^3} - \frac{A_1\cosh(ay)(a(-7+a^2(-1+y^2))\cosh(a) + (7-a^2(-6+y^2))\sinh(a))}{8(\text{acosh}(a) - \sinh(a))^3}$$

$$v^{(2)} = \frac{a^2k_1{S_1}^2\cosh(a)(2ay(6+\cosh(2a)) + 14y\cosh(ay)(-\text{acosh}(a) + \sinh(a)) - 7y\sinh(2a))}{8(\text{acosh}(a) - \sinh(a))^3} + \frac{2a^3k_1{S_1}^2\cosh(a)(a(-1+y^2)\cosh(a) - (-6+y^2)\sinh(a))\sinh(ay)}{8(\text{acosh}(a) - \sinh(a))^3}$$

where

$$A_1 = a^2k_1S_1(-1+2S_1x)\cosh(a).$$

$$\begin{aligned} p^{(2)} = {} & A_2(16a^2Da\cosh(2ay)(\text{acosh}(a) - \sinh(a)) \\ & - 2A_3\cosh(ay)(a(-7+a^2(-1+y^2))\cosh(a))) \\ & - 2A_2A_3\cosh(ay)(7-a^2(-6+y^2))\sinh(a) \\ & + A_2(1+\lambda_1)\cosh(a)(2a(6+\cosh(2a))) \\ & + 7A_2(1+\lambda_1)\cosh(a)\sinh(2a) \\ & + 10ayA_2A_3(\text{acosh}(a) - \sinh(a))\sinh(ay) + F(y) \end{aligned}$$

where $A_2 = \dfrac{a^2k_1S_1(-x+S_1x^2)}{16Da(1+\lambda_1)(\text{acosh}(a) - \sinh(a))^3}$, $A_3 = (-1+a^2Da-\lambda_1)\cosh(a)$.

$$\begin{aligned} F'(y) = {} & (A_4 + A_5x + A_6x^2)y\cosh(ay) + A_7y \\ & + (A_8 + (A_9 + A_{10}x)x + (A_{11} + A_{12}x + A_{13}x^2)y^2) \\ & \times \sinh(ay) + (A_{14} + (A_{15} + A_{16}x)x)\sinh(2ay) \\ p^{(2)} = {} & (A_{17} + (A_{18} + A_{19}x)x) \\ & \times \cosh(2ay) + (A_{20} + A_{21}y^2)\cosh(ay) \\ & + (A_{22} + A_{23}x)x + (A_{24}y + A_{25}\sinh(ay))y + p_0{}^{(2)} \end{aligned}$$

where $p_0{}^{(2)}$ is the pressure at the entrance of the slit.

$$\bar{p}^{(2)}(x) = A_{26} + (A_{27} + A_{28}x)x$$

$$\Delta\bar{p}^{(2)}(L) = -\frac{a^2k_1LS_1(-1+LS_1)\cosh(a)(4a(3+2Da+3\lambda_1) + 2a(1-4Da+\lambda_1)\cosh(2a))}{16Da(1+\lambda_1)(\text{acosh}(a) - \sinh(a))^3} - \frac{a^2k_1LS_1(-1+LS_1)\cosh(a)(-7+8a^2Da-7\lambda_1)\sinh(2a)}{16Da(1+\lambda_1)(\text{acosh}(a) - \sinh(a))^3}$$

$$T_{xx}{}^{(2)} = -p_0{}^{(2)} + (A_{29} + A_{30}x + A_{31}x^2)\cosh(2ay) + A_{32} + (A_{33} + A_{34}y^2)\cosh(ay) + A_{35}y^2 + (A_{36} + A_{37}x)x + A_{38}y\sinh(ay)$$

$$T_{xy}{}^{(2)} = (-1 + 2S_1x)(A_{39}y\cosh(ay) + (A_{40} + A_{41}y^2)\sinh(ay) + A_{42}\sinh(2ay))$$

$$T_{yy}{}^{(2)} = -p_0{}^{(2)} + A_{43} + A_{44}\cosh(2ay) + (A_{45} + A_{46}y^2)\cosh(ay) + (A_{47} + A_{48}x)x + A_{49}y^2 + A_{50}y\sinh(ay)$$

$$T_{xx}{}^{(2)} - T_{yy}{}^{(2)} = (A_{51} + A_{52}x + A_{53}x^2) \times \cosh(2ay) + A_{54} + (A_{55} + A_{56}x)x + (A_{57} + A_{58}y^2) \times \cosh(ay) + A_{59}y\sinh(ay)$$

where A_4, A_5, A_6,…,A_{59} are all constants depending upon k_1, S_1 and a.

$$\psi = (C_1 + C_2x)y + (C_3 + C_4x)y^3 + (C_5y + C_6y^3 + C_7xy + C_8xy^3)\cosh(ay) + (C_9 + C_{10}y^2 + C_{11}y^4 + x(C_{12} + C_{13}y^2 + C_{14}y^4)) \times \sinh(ay) + (C_{15} + C_{16}x)\sinh(2ay),$$

$$u = C_{17} + C_{18}x + C_{19}y^2 + C_{20}xy^2 + C_{21}\cosh(2ay) + (C_{22} + C_{23}y^2 + C_{24}y^4)\cosh(ay) + (C_{25} + C_{26}y^2 + C_{27}y^4)x\cosh(ay) + (C_{28}y + C_{29}y^3 + (C_{30}y + C_{31}y^3)x)\sinh(ay),$$

$$v = (C_{32} + C_{33}y^2)y + (C_{34} + C_{35}y^2)y\cosh(ay) + (C_{36} + C_{37}y^2 + C_{38}y^4)\sinh(ay) + +C_{39}\sinh(2ay),$$

$$p - p_0 = C_{40}y^4 + C_{41}y^2 + C_{42}xy^2 + C_{43}x + C_{44}x^2y^2 + C_{45}x^2 + (C_{46} + C_{47}y^2 + C_{48}y^4)\cosh(ay) + (C_{49} + C_{50}x + C_{51}xy^2 + C_{52}x^2 + C_{53}y^2 + C_{54}x^2y^2)\cosh(2ay) + (C_{55}y + C_{56}y^3)\sinh(ay) + (C_{57}xy + C_{58}x^2y + C_{59}y)\sinh(2ay),$$

$$\bar{p}(x) = C_{60} + C_{61}x + C_{62}x^2,$$
$$\Delta\bar{p}(L) = (C_{63}L + C_{64}L)L.$$

$$T_{xx} = C_{65} + C_{66}x + C_{67}y^2 + C_{68}y^4 + C_{69}xy^2 + C_{70}x^2 + C_{71}x^2y^2 + (C_{72}y + C_{73}y^3)\sinh(ay) + (C_{74} + C_{75}y^2 + C_{76}x + C_{77}xy^2 + C_{78}x^2 + C_{79}x^2y^2) \times \cosh(2ay) + (C_{80} + C_{81}y^2 + C_{82}y^4)\cosh(ay) + (C_{83}y + C_{84}x + C_{85}x^2)\sinh(2ay) - p_0,$$

$$T_{xy} = (C_{86} + C_{87}x)y + (C_{88} + C_{89}x)y\cosh(2ay) + (C_{90} + C_{91}y^2 + C_{92}x + C_{93}xy^2)y\cosh(ay) + (C_{94} + C_{95}y^2 + C_{96}y^4 + C_{97}x + C_{98}xy^4 + C_{99}xy^2)\sinh(ay) + (C_{100} + C_{101}y^2)\sinh(2ay) + (C_{102} + C_{103}y^2)x\sinh(2ay),$$

$$T_{yy} = C_{104} + C_{105}x + C_{106}x^2 + C_{107}y^2 + C_{108}y^4 + (C_{109} + C_{110}y^2)\cosh(2ay) + C_{111}y\sinh(2ay) + (C_{112} + C_{113}y^2 + C_{114}y^4)\cosh(ay) + (C_{115} + C_{116}y^2)y\sinh(ay) - p_0,$$

$$T_{xx} - T_{yy} = C_{117} + C_{118}x + C_{119}x^2 + C_{120}y^2 + C_{121}xy^2 + C_{122}x^2y^2 + (C_{123} + C_{124}y^2 + C_{125}y^4)\cosh(ay) + (C_{126} + C_{127}x + C_{128}x^2 + C_{129}y^2 + C_{130}xy^2 + C_{131}x^2y^2) \times \cosh(2ay) + (C_{132} + C_{133}y^2)y\sinh(ay) + (C_{134} + C_{135}x + C_{136}x^2)y\sinh(2ay),$$

$$T_{wall} = T_{xy}|_{y=1} = C_{139}(-1 + 2S_1x).$$
$$u_{\max} = C_{137} + C_{138}x,$$
$$v_{\max} = S_1$$

where $p_0{}^{(1)} + p_0{}^{(2)} + p_0{}^{(3)} = p_0$ and C_1, C_2, C_3,…,C_{139} are all constants.

References

[1] Conry T F 1984 *ASME, J. Tribol.* **106** 275
[2] Oliver D R 1988 *J. Non-Newton Fluid Mech.* **30** 185
[3] Spikes H A 1994 *Proc. Inst. Mech. Eng. J.* **208** 3
[4] Sawyer W G and Tichy J A M 1998 *J. Tribol.* **120** 622
[5] Zhang L, Bhatti M M, Marin M and Mekheimer S K 2020 *Entropy* **22** 1070
[6] Abo-Elkhair R E, Bhatti M M and Mekheimer K S 2021 *Int. Commun Heat Mass* **123** 105228
[7] Ali Z, Zeeshan A, Bhatti M M, Hobiny A and Saeed T 2021 *Arab. J. Sci. Eng.* **46** 6039
[8] Bhatti M M 2021 *Inventions* **6** 28
[9] Shehzad N, Zeeshan A and Ellahi R 2018 *Commun. Theor. Phys.* **69** 655
[10] Shaheen S, Maqbool K, Ellahi R and Sait S M 2021 *Commun. Theor. Phys.* **73** 035006
[11] Ellahi R, Sait S M, Shehzad N and Ayaz Z 2020 *Int. J. Numer. Methods Heat Fluid Flow* **30** 834
[12] Alamri S Z, Ellahi R, Shehzad N and Zeeshan A 2019 *J. Mol. Liq.* **273** 292
[13] Ahmad S, Nadeem S and Muhammad N 2019 *Commun. Theor. Phys.* **71** 344
[14] Bou-Saïd B and Kane M 2005 *J. Tribol.* **127** 575
[15] Wang F C and Jin Z M 2005 *J. Tribol.* **127** 729
[16] Gao L M, Meng Q E, Wang F C, Yang P R and Jin Z M 2007 *Proc. Inst. Mech. Eng. J.* **221** 133
[17] Barath S, Shokouhmand H, Ajarostaghi S S M and Nikian M 2018 *Int. J. Therm. Sci.* **134** 370
[18] Bird R B, Armstrong R C and Hassager O 1987 *Dynamics of Polymeric Liquids.* (*Fluid Mechanics* vol 1) 2nd edn (Hoboken, NJ: Wiley)
[19] Baris S 2003 *Turk. J. Eng. Environ. Sci.* **27** 73
[20] Yamamoto T, Suga T, Nakamura K and Mori N 2004 *J. Fluids Eng.* **126** 148
[21] Nallapu S and Radhakrishnamacharya G 2014 *Int. J. Eng. Math.* **2014** 713831
[22] Reddappa B, Sreenadh S and Naidu K K 2015 *Adv. Appl. Sci. Res.* **6** 69
[23] Mirzakhalili E and Nejat A 2015 *J. Fluids Eng.* **137** 031205
[24] Nadeem S, Hussain A and Majid K 2010 *Z. Naturforsch.* A **65** 540

[25] Hayat T, Awais M, Asghar S and Hendi A A 2011 *J. Fluids Eng.* **133** 061201
[26] Turkyilmazoglu M 2016 *Z. Naturforsch.* A **71** 549
[27] Turkyilmazoglu M 2009 *Phys. Fluids* **21** 106104
[28] Turkyilmazoglu M 2009 *J. Appl. Math. Mech.* **89** 490
[29] Baragh S, Shokouhmand H and Ajarostaghi S S M 2019 *Int. J. Therm. Sci.* **137** 388
[30] Farooq J, Chung J D, Mushtaq M, Lu D, Ramazan M and Farooq U 2018 *Results Phys.* **11** 861
[31] Ajarostaghi S S M, Delavar M A and Poncet S 2020 *J. Therm. Anal. Calorim.* **140** 1321
[32] Bhatti K, Bano Z and Siddiqui A M 2018 *Eur. J. Pure Appl.* **11** 937
[33] Lin Y and Yang M 2020 *Commun. Theor. Phys.* **72** 095003
[34] Langlois W E 1963 *Trans. Soc. Rheol.* **7** 75
[35] Mehboob H, Maqbool K, Siddiqui A M and Ullah H 2020 *J. Fluids Eng.* **143** 021303
[36] Siddiqui A M and Azim Q A 2020 *Chin. J. Phys.* **64** 264
[37] Ullah H, Sun H, Siddiqui A M and Haroon T 2019 *J. Appl. Anal. Comput.* **9** 140
[38] Haroon T, Siddiqui A M and Shahzad A 2016 *Appl. Math. Sci.* **10** 795
[39] Mullins L J, Conway B R, Menzies R I, Denby L and Mullins J J 2016 *Models Mech.* **9** 1419
[40] Siddiqui A M, Siddiqa S and Naqvi A S 2018 *J. Appl. Comput. Math.* **7** 1